Materials Horizons

Ductile Adhesive Elastomers with Force-Triggered Ultra-High Adhesion Strength

Journal:	*Materials Horizons*
Manuscript ID	MH-COM-08-2023-001280.R1
Article Type:	Communication
Date Submitted by the Author:	04-Nov-2023

Complete List of Authors:	Zhao, Xiao; GCP Applied Technologies Inc, Research and Development; Oak Ridge National Laboratory Physical Sciences Directorate, Chemical Sciences Division Demchuk, Zoriana; Oak Ridge National Laboratory Physical Sciences Directorate, Chemical Sciences Division Tian, Jia; Beijing University of Chemical Technology, School of Materials Science and Engineering Luo, Jiancheng; Oak Ridge National Laboratory, Physical Sciences Directorate; university of akron Li, Bingrui ; University of Tennessee Knoxville, Bredesen Center for Interdisciplinary Research and Graduate Education Cao, Ke; Oak Ridge National Laboratory Physical Sciences Directorate, Chemical Sciences Division Sokolov, Alexei; University of Tennessee Knoxville College of Engineering, Department of Chemistry and Physics & Astronomy Hun, Diana; Oak Ridge National Laboratory Saito, Tomonori; Oak Ridge National Laboratory, Chemical Sciences Division Cao, Pengfei; Beijing University of Chemical Technology, School of Materials Science and Engineering

Ductile Adhesive Elastomers with Force-Triggered Ultra-High Adhesion Strength

New Concepts

In this manuscript, we pioneer the incorporation of the unique "on-demand" adhesion feature into functional ductile elastomers, which is completely different from regular pressure-sensitive adhesives. The adhesion feature is easily triggered by mechanical force when needed, and such feature can effectively reduce the energy cost, prevent the damage and improve the convenience during handling. After a force trigger and curing process, it exhibits the peel strength and lap shear strength of 1.2×10^4 N/m and 7.8×10^3 kPa, respectively, that tops the reported adhesive advanced functional elastomers. The rheology properties of the adhesive elastomer after curing reveal that the excellent ability to adapt to rough surfaces and the reinforced elastomer modulus contribute to the ultra-high adhesion strength. The unique "on-demand" adhesion of functional elastomer along with the demonstrated prefab module application will shed a light on fabricating functional polymeric materials with different applications.

Communication

Ductile Adhesive Elastomers with Force-Triggered Ultra-High Adhesion Strength

Received 00th January 20xx,
Accepted 00th January 20xx

DOI: 10.1039/x0xx00000x

Xiao Zhao[a], Zoriana Demchuk[a], Jia Tian[b], Jiancheng Luo[a], Bingrui Li[c], Ke Cao[a], Alexei P. Sokolov[a,d], Diana Hun[e†], Tomonori Saito[a††], and Peng-Fei Cao[b†††]

Elastomers play a vital role in many forthcoming advanced technologies that in which their adhesive properties determine materials' interface performances. Despite great success in improving adhesive properties of elastomers, permanent adhesives tend to stick to the surfaces prematurely or result in poor contact depending on the installation method. Thus, elastomers with on-demand adhesion that is not limited to being triggered with UV light or heat, which may not be practical for scenarios that do not allow an additional external source, provide a solution to various challenges in conventional adhesive elastomers. Herein, we report a novel, ready-to-use, ultra high-strength, ductile adhesive elastomer with an on-demand adhesion feature that can be easily triggered by a compression force. The precursor is mainly composed of a capsule-separated, two-component curing system. After a force-trigger and curing process, the ductile adhesive elastomer exhibits a peel strength and lap shear strength of 1.2×10^4 N/m and 7.8×10^3 kPa, respectively, which exceed the reported values for advanced ductile adhesive elastomers. The ultra-high adhesion force is attributed to the excellent surface contact of the liquid-like precursor and to the high elastic modulus of the cured elastomer that is reinforced by a two-phase design. Incorporation of such on-demand adhesion into an elastomer enables a controlled delay between installation and curing so that these can take place at their individual ideal conditions, effectively reducing the energy cost, preventing failures, and improving handling.

1. Introduction

Elastomers are rooted in every aspect of our daily life as they are used in consumer and industrial products like sealants, vibration dampers, tires, footwear, toys, furniture, packaging, adhesives, and additives, etc. They play a vital role in forthcoming advanced technologies, including but not limited to flexible displays, wearable devices, soft robotics, invasive surgery, building construction, solid-state batteries, and artificial human skin[1-9]. Chemical or physical crosslinking of the natural rubber, polyurethane, polybutadiene, neoprene, co-polyester, or silicone-based polymers, allow ductile elastomers to possess properties like good extensibility, decent elastic modulus, remarkable recoverability (low mechanical loss), and excellent chemical resistance[10-15]. Aside from these fundamental properties, advanced ductile elastomers can have other special features such as self-healing, ultra-chemical stability, dielectric response, thermal or magnetic sensitivity, and high optical transparency. These features are typically accomplished by the introduction of single or multiple dynamic bonds, addition of functional additives, formation of micro-phase separations, manipulation of molecular topology, or engineering into special geometry or composites[16-33]. For example, a graphene-containing liquid crystalline elastomer enabled photo-actuation by absorbing near-infrared light and triggering nematic-to-isotropic phase transition, achieving high actuation force and reversible flexibility[22]. The interpenetration of the conductive PEDOT:PSS and zwitterionic poly(HEAA-co-SBAA) networks allowed fabrication of a fully polymeric strain sensor with high mechanical recovery and strong surface adhesion[34]. A super stretchable (≈ 2260%) and recyclable polyurethane elastomer was recently achieved by introducing dynamic π-π motifs and phosphorus-containing moieties[15]. An ionic conducting elastomer with autonomous self-healability at 5 °C also afforded to serve as an efficient protecting layer for the stable cycling of lithium-metal batteries at relatively low temperatures[35].

With significantly growing demands of functional ductile elastomers in advanced technologies, their adhesive properties play a critical role in determining the lifetime and reliability in the designated fields[36-45]. The incorporation of intermolecular interactions is an important strategy to improve the adhesive properties of elastomers. For example, Chen *et al*. and Tan *et al*. independently demonstrated that the incorporation of a small amount of hydrogen-bonding 2-ureido-4[1H]-pyrimidinone (UPy) group enhanced adhesion force of the elastic materials to organic and inorganic substrates for finger strain sensors and soft robot

[a] *Chemical Sciences Division, Oak Ridge National Laboratory, Oak Ridge, TN 37830, USA.*
[b] *State Key Laboratory of Organic-Inorganic Composites, Beijing University of Chemical Technology, Beijing 100029, China.*
[c] *The Bredesen Center for Interdisciplinary Research and Graduate Education, University of Tennessee, Knoxville, TN 37996, USA.*
[d] *Department of Chemistry, University of Tennessee, Knoxville, TN 37996, United States.*
[e] *Buildings and Transportation Science Division, Oak Ridge National Laboratory, Oak Ridge, TN 37830, USA.*
† Email: hunde@ornl.gov
†† Email: saitot@ornl.gov
††† Email: caopf@buct.edu.cn
Electronic Supplementary Information (ESI) available. See DOI: 10.1039/x0xx00000x

actuators[46, 47]. By using the monomer of 4-acryloyl morpholine that intrinsically possesses hydrogen-bonding interactions, a self-adhesive ionic elastomer was synthesized that exhibits peel strength of 28 N/m on a paper substrate and allows the assembly of stretchable motion energy harvester[48]. The addition of 15 mol. % dopamine increased the adhesive strength of urethane elastomers from 30 to 71 kPa when used as bio-interfacial electrodes[27]. A series of self-healable, adhesive elastomers were also demonstrated to show ultra-high adhesion force, even on dusty surfaces (3488 N/m), by simply mixing the self-healing polymer and commercially available curable elastomers[25]. Aside from physical interactions, adjusting the surface geometries in micro-scale also facilitates the adhesion of elastomers to various substrates. For example, the adhesion force of poly(dimethyl siloxane) (PDMS) elastomer to the human skin was improved by 10 times due to the enhanced Van der Waals force *via* the formation of micrometer-sized wrinkles on the elastomer, which was rendered by the addition of 0.004 wt. % ethoxylated poly(ethyleneimine)[49]. By controlling the interfacial interaction-induced surface wrinkling between poly(L-lactide) and PDMS, a single-component micro-wrinkled PDMS elastomer was shown to have tunable adhesion capabilities[50]. Although the enhancement of adhesion force has been demonstrated for functional ductile elastomers, few have the flexibility of on-demand control of when full-adhesion occurs. Therefore, they often require extra protection and labor before and during the installation onto the target substrate as well as lack convenience during handling. Hence, developing a force-triggered on-demand feature is a more practical, one-step solution for scenarios such as flexible devices or prefab construction that will significantly benefit from having a controlled delay between installation and adhesion.

Microencapsulation technology, originated from the pursuit of a protection envelop that can control the exchange of materials like a living cell, has been widely adapted in different applications such as extrinsic extrinsic self-healing[51-53], food protection[54], drug delivery[55], wound management[56, 57], photovoltaic protection[58], thermal sensitive adhesives[59], etc. In general, the active ingredients encapsulated in the micro shells are released out continuously at a slow rate or completely upon shell rupture. The latter could be triggered by physical stimuli, such as macroscopic fracture[51, 60, 61], temperature[59, 62], ultra-sound[63], and compression[64-66]. Among above, the compression force is the most convenience trigger, as no thermal or acoustic equipment is required. Also, it allows a universal breakage of microcapsules that triggers adhesion in comparison to the crack or fracture that only triggers local healing.

Herein, we demonstrate a novel design for an on-demand, ultra-high strength ductile adhesive elastomer, whose adhesion is triggered by compression force. This triggering method is more robust than the moisture or light-trigger curing, since such factors are normally difficult to avoid at ambient condition[67]. In general, we select a urea-based elastomer that is fabricated by methylene diphenyl diisocyanate (MDI)-prepolymer and polypropylene glycol (PPG)-diamine as resin and curing agents, respectively. The on-demand feature is achieved through a compression force to break the encapsulated resin agent and trigger the curing reaction, as illustrated in Figure 1. Notably, our design is different from the two/multi-component self-healing[51, 60, 61], of which our adhesive elastomer is homogenously cured with mechanical performance and interfacial binding significantly improved, whereas the microencapsulation self-healing aims at repeatedly restoring the local damage. Also, this adhesive elastomer is different from the conventional pressure-sensitive adhesives, as the latter involves merely physical tacking and typically low adhesion on rough surfaces which will be discussed later. Here, the combination of the intrinsic adaptability on the receiving substrate, *i.e.*, micro-scale geometry adaption, and the reinforced mechanical strength enabled the developed ductile adhesive elastomer to achieve an ultra-high adhesion force with

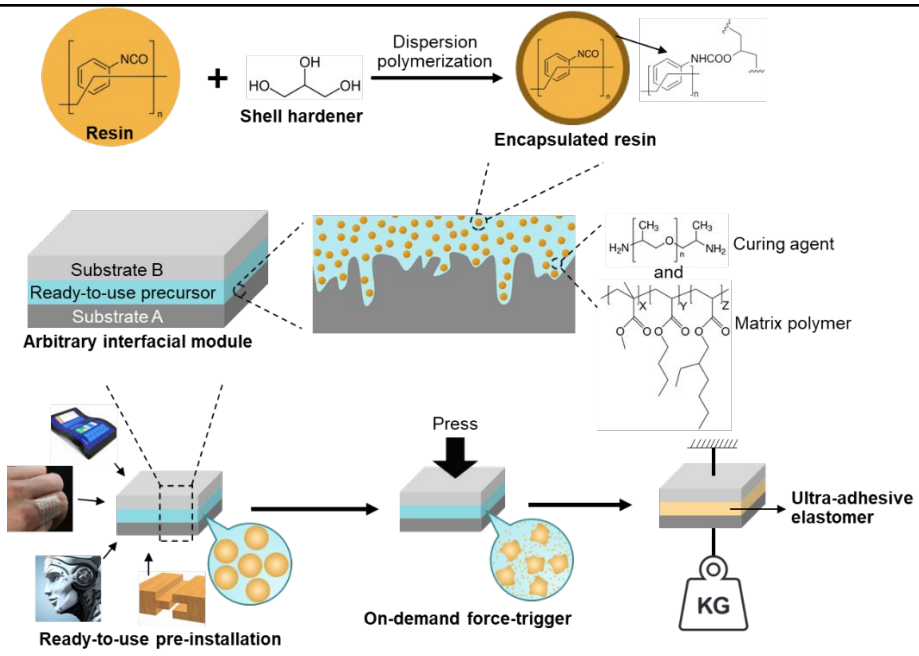

Figure 1. Illustration of the on-demand ultra-high adhesion formation of the ready-to-use precursor and its preparation process. The resin, curing agent, and matrix polymer are MDI-prepolymer, PPG-diamine, and acrylates copolymer, respectively.

peel strength and adhesion strength exceeding the magnitude of 10^4 N/m and 10^3 kPa, respectively. To the best of our knowledge, the adhesion force of such elastomers is outstanding from that of the currently reported ductile adhesive elastomers. With such ultra-high adhesion force and on-demand adhesion that can be conveniently applied by human force, it is anticipated that such ductile adhesive elastomer can be used in a great variety of applications.

2. Results and discussion

The ready-to-use elastomer precursor is composed of an encapsulated MDI-prepolymer and PPG-diamine, as reactive and curing agents, respectively, along with a matrix polymer of methyl methacrylate-butyl acrylate-ethylhexyl acrylate random copolymer poly(MMA-*r*-BA-*r*-EHA), as depicted in Figure 1. The reactive and curing agents were selected based on pre-screens of curing rate from various two-component elastomer systems, between a reactive agent, including bisphenol-A-diglycidyl ether, EPON 8111, hexamethylene diisocyanate (HDI) prepolymer, and MDI-prepolymer, and a curing agent, including polyethyleneimine (PEI), PPG-triamine, PPG-diamine, and PPG-di-OH[68-70]. A suitable curing rate allows adequate time for the substrates that will be adhered to each other to be adjusted while requires not too long waiting time (< 2 hour). The pre-screen tests (SI, Table S1) showed that neither diol- nor PEI-type curing agent cured in a reasonable rate. Additional PPG-triamine is required to slow down the PEI-type curing agent, which adds the complexity. Regarding the reactive agents, epoxy-based agents could not be cured merely with diamine/triamine, and HDI-prepolymer cured too fast with diamine in which additional diol is required for suitable curing rate. Therefore, the combination of MDI-prepolymer and PPG-diamine was the most suitable among them, considering their curing rate as well as the raw materials availability and the ability to be scaled up. Both MDI-prepolymer and PPG-diamine contain reactive terminal groups with sufficient chain length to attain flexibility for the obtained elastomer without harming its cohesive strength[71-73]. The adhesive random copolymer, *i.e.*, poly(methyl methacrylate-*r*-butyl acrylate-*r*-2-ethylhexyl acrylate) was utilized as a polymer matrix, which improves the longevity and interfacial adhesion for the elastomers, especially before the force-triggered curing.

The microencapsulation process is established[52, 53], and the encapsulated MDI-prepolymer was synthesized using a single-step dispersion polymerization between MDI-prepolymer and glycerol, as illustrated in Figure 1. Specifically, the gum Arabic, dodecyl trimethylammonium bromide (DTAB), and glycerol were used as surfactant, segregation aid, and shell extender with the synthesis protocol demonstrated in Scheme S1. The well-dispersed MDI-prepolymer droplets were partially crosslinked by glycerol to form the shell of the microcapsules[68], sealing the unreacted MDI-prepolymer inside. It is noteworthy that the addition of a cationic surfactant, i.e., DTAB, introduces columbic repulsion on the surface of the microcapsules that effectively prevents microcapsule aggregation (SI, Figure S1), which increases the robustness of microcapsules during handling. The characteristic chemical structure of the shell was demonstrated by FT-IR as shown in Figure 2A. The peaks at 1235 and 1310 cm^{-1} correspond to the urethane ester bond formed between isocyanate groups from MDI-prepolymer and hydroxyl units in glycerol[74, 75]. Moreover, a significant peak at 2250 cm^{-1} that corresponds to the isocyanate group was observed for both broken microcapsules and MDI-prepolymers[76], indicating the presence of a significant amount of reactive isocyanate groups inside the microcapsule. The DSC result (SI, Figure S2) of the MDI-prepolymer-containing microcapsule also confirmed the presence of an isocyanate group. The diameter of microcapsule was tunable from 10 to 900 μm by changing the mixing speed of the agitator during dispersion. The result of microcapsule diameters *vs*. agitating speeds is provided in Figure 2B, along with the representative optical microscope images for samples prepared at 300 and 1000 RPM. Tunning the size of microcapsules can potentially affect two important factors: 1) the force required to break the microcapsules and trigger the curing reaction; 2) the dispersion of released reactive agents in the polymer matrix. The scanning electron microscope (SEM) results (SI, Figure S3) clearly showed that the microcapsules were able to be broken by sufficient external force.

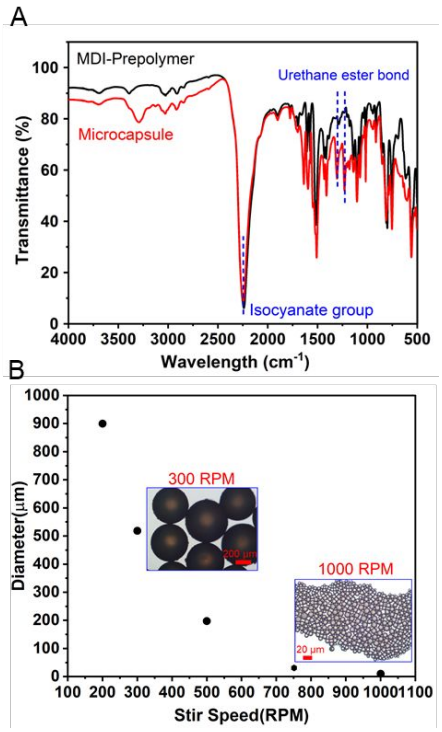

Figure 2. A) FT-IR spectra of MDI-prepolymer reagent and encapsulated MDI-prepolymer. B) Diameter of the synthesized microcapsules *vs*. the agitation speed during emulsion polymerization, along with visualizations of the microcapsules by optical microscope.

The matrix polymer was synthesized by a free-radical random copolymerization of methyl methacrylate (MMA), butyl acrylate (BA), and ethylhexyl acrylate (EHA)[77]. The random copolymer with the feed ratio of MMA being 35 mol. % was selected due to its suitable glass transition temperature (T_g), which optimized the adhesion and self-healability; the BA to 2-EHA feed ratio was 2:1 by weight. The chemical structure of the synthesized matrix polymer was confirmed by ^{1}H NMR (Figure 3A) and FT-IR spectra (SI, Figure S4), where the composition of the MMA unit was 29 mol. %, as calculated by integrating the corresponding ^{1}H NMR peaks,

consistent with the feed ratio. The molecular weight (M_n) of the copolymer was 23.6 kDa as measured by GPC, and the relatively

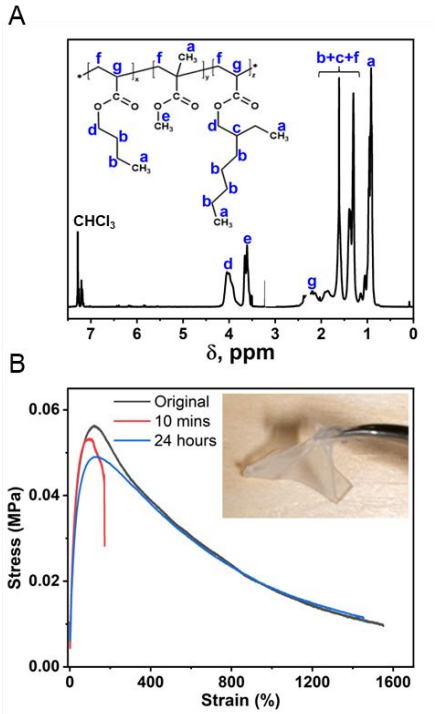

Figure 3. A) ^{1}H-NMR spectrum of the matrix polymer with characteristic chemical shift peaks marked on the chemical structure. B) Tensile results of the cut matrix polymer that self-healed for 10 min and 24 h in comparison to the original uncut material.

broad polydispersity (PDI = 2.62) is typical for such random radical copolymerization. The low T_g (-33 °C using DSC, SI Figure S5) manifested the rubbery nature of such copolymer over a wide temperature range. The dynamic mechanical analysis (DMA) result (SI, Figure S6) clearly demonstrated that the modulus of the matrix polymer was around 2-5 MPa at room temperature, which is important for good interfacial adhesion. The tensile test exhibited excellent extensibility of such matrix polymer with elongation before breaks over 1500%. Having low T_g, high flexibility and adhesion also enables the self-healing capability. The self-healability was examined by mechanically cutting the cured adhesive into two parts and subsequently arranging them so that they were in contact with each other. After a 24-hour healing process at ambient conditions, the matrix polymer could fully recover its mechanical property as shown in Figure 3B.

The ready-to-use precursor was further formulated of the synthesized microcapsules with encapsulated MDI-prepolymer, PPG-diamine, and matrix polymer. Specifically, we chose the microcapsules that were synthesized under 300 RPM for the following results. The initial formulation of the elastomer precursor contained 60 wt. % microcapsules, 30 wt. % PPG-diamine, and 10 wt. % matrix polymer, which afforded the cured elastomer with adhesion force in the order of magnitude of 10^3 N/m (SI, Figure S7). To optimize the composition ratios for the maximal reaction extent, the isocyanate content in the microcapsules with a diameter of 520 μm was calculated through a titration using bromophenol and an excess quantity of amines (see Scheme S2 for the titration protocol). Based on the calculated result (isocyanate content 20.9 wt. %), we optimized the composition of the ready-to-use precursor to be 50 wt. % encapsulated MDI-prepolymer, 40 wt. % PPG-diamine and 10 wt. % matrix polymer, so the unreacted excess agents was minimized. Such formulation was utilized for further studies.

To better control the force during the pre-installation process and on-demand curing, we loaded the precursor to a customized shallow groove-shaped container. The curing reaction was then triggered by applying a 500 N compression force for 30 seconds on a 10 cm^2 flat surface, and such short dwell time was sufficient to allow a homogenous force distribution against the stress relaxation of the precursor. The 500 N compression force was selected based on a preliminary screening of the breaking state of microcapsules and the resultant peel strength (SI, Table S2, and Figure S8) against different compression forces. A significant increase (500%) of peel strength was observed for 500 N, indicating the sufficient breakage of microcapsules. Notably, this does not necessarily mean that all microcapsules were broken by such compression force, because there might be a small portion of smaller microcapsules requiring larger compression force. However, the amount of such small portion was inadequate for significant macroscopic defects that influence the cohesive strength of elastomer. Such a hypothesis was indirectly proved by the similar tests for microcapsules synthesized at 200 RPM (Table S3 and Figure S9), where the critical inflection region became less steep due to the broader distribution of microcapsule size. On the other hand, the microcapsules synthesized

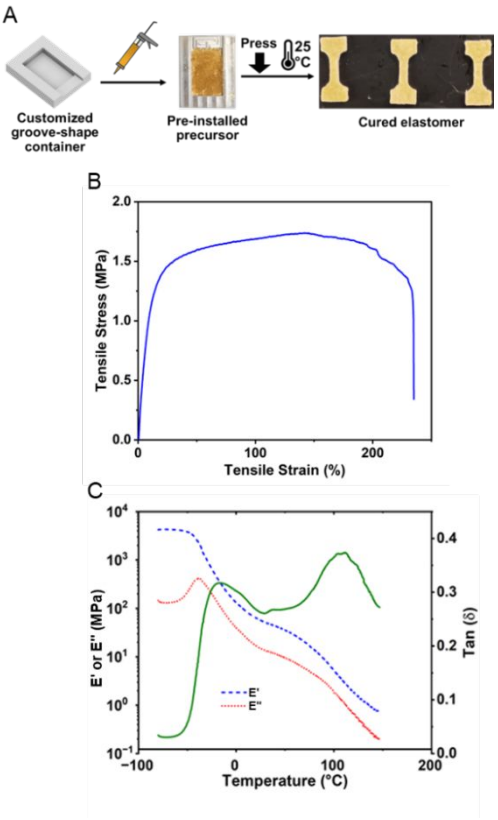

Figure 4. A) Protocols to cure the pre-installed precursor and preparation of samples for tensile tests. B) Tensile result of the ductile adhesive elastomer that was cured at 25 °C for three days. C) Dynamic modulus and phase angle of the cured ductile adhesive elastomer by temperature sweep using DMA.

at 200 RPM exhibit inferior adhesion performance compared to that from the 300-RPM. The advantage of microcapsules synthesized at 200 RPM is that a smaller trigger force, 150N, was sufficient to trigger the curing. Obviously, the triggering force could be further tuned by varying the microcapsule sizes and adjusting the precursor formulation, whereas this fine-tuning confronted the challenge as the capsule thickness needed to be proportionally scaled against its size. After compression, the sample was cured for three days for complete cure at 25 °C in a temperature-controlled chamber prior to being processed for the tensile test (Figure 4A). Herein, the tensile test was performed at a tensile rate of 1 mm/s with the result plotted in Figure 4B. The cured elastomer illustrated a maximum tensile stress of 1.75 MPa and an elongation at breakage of 223 %, a decent mechanical performance in comparison with advanced ductile adhesive elastomers[48, 49, 78-81].

The viscoelasticity of the cured elastomer was further investigated by temperature sweep using DMA as shown in Figure 4C. At temperatures below -35 °C, a typical glassy modulus around 4.3 GPa was observed. As the temperature increases, the result of phase angle clearly indicated a broad transition from -25 °C to 0 °C, due to the devitrification of the cured ductile polyurea elastomer network. Herein, longer polyether chains were selected between crosslinks to avoid high rigidity, and therefore the T_g of the network was relatively low compared to rigid polyurea materials[82]. From 0 to 75 °C, a temperature-dependent elastic region was demonstrated for

cured elastomers, mainly due to the strongly temperature-dependent mechanical strength of matrix polymer. The characteristic elastic modulus is around 40 MPa, which is at least 10 times higher than the typical rubber-state modulus[83-87]. The high elastic modulus intrinsically enhances the cohesive strength of the adhesive elastomer[88-91]. Such enhancement was presumably caused by the mechanical reinforcement of the highly crosslinked microcapsule shells phase separated in the elastomer matrix[31, 92-94]. The existence of a phase separation was indicated in $\tan(\delta)$ spectrum (Figure 4C) as a high-temperature transition peak at 110 °C, and such temperature agreed with the T_g of crosslinked microcapsules (SI, Figure S2).

As mentioned earlier, the novel design achieves the on-demand, ultra-high adhesion strength. The on-demand feature is important especially when the ductile adhesive elastomeric materials need controlled delay between the installation and adhesion, which often requires exterior protection and lacks flexibility of the installation. Some previous research (even current commercial products) demonstrated the moisture- or light-triggered adhesion, whereas such triggering factors were easily disturbed by ambient humidity or light[67]. Comparatively, the mechanical-force trigger can be easily secured at ambient conditions and readily applied by end users. Herein, the on-demand feature is easily achieved by applying a uniform compression force on the pre-installed ready-to-use precursor. Such a strategy is different from the well-reported pressure-sensitive adhesives, although the latter also has the on-demand feature. The regular pressure-sensitive adhesives involve no chemical changes during the installation, and the external force triggers a viscoelastic change to tack to the substrate. Therefore, its crosslinking extent and matrix rigidity are limited, as the peel strength is around 10^3 N/m[95-97]. Moreover, the thickness of pressure-sensitive adhesives is often less than 100 μm to retain the shear resistance[98-100], which limits its performance on various rough surfaces. On the contrary, our force-triggering strategy involves a chemical curing process that provides at least 10 times higher strength to adhere to the substrate and maintain the cohesion, as is shown below.

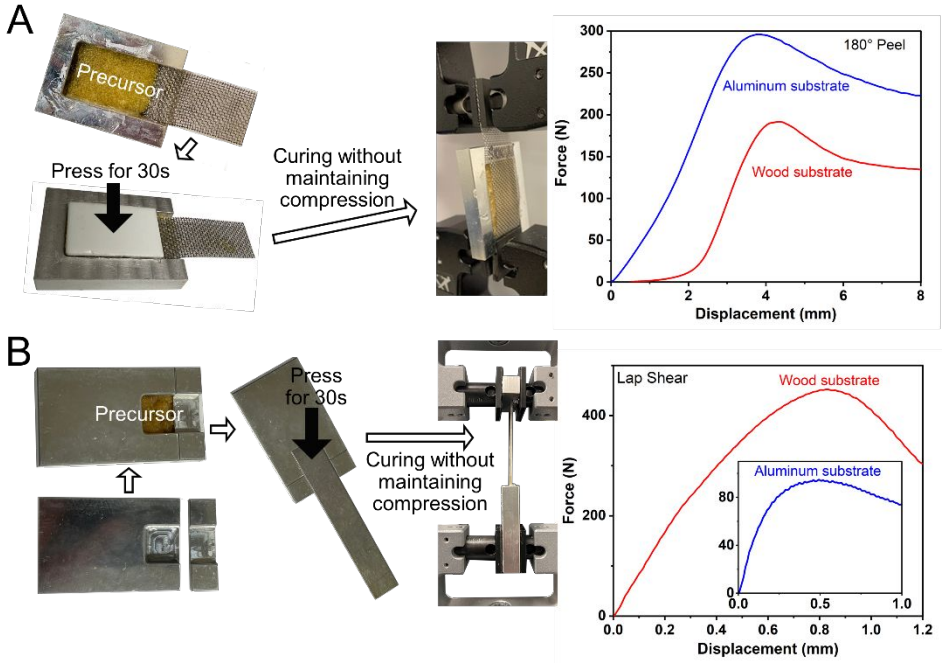

Figure 5. A) Peel result of the cured ductile adhesive elastomer using a 180° peel setup. B) Tensile result of the cured ductile adhesive elastomer using a lap shear setup.

Moreover, the flexibility of the ready-to-use precursor and

unlimited choices of thickness facilitates versatile adaption with various surface conditions.

The adhesion force of ductile adhesive elastomer was studied by the peel and lap shear strength to benchmark the reported ductile adhesive elastomers. Here, we used the customized test kits that contain an embedded groove, similar to the container illustrated in Figure 4A, and the testing methods comply with ASTM C794 and C961 standards. The test results of peel strength and lap shear on both aluminium and wood substrates, along with pictures of the testing setup, are shown in Figures 5A and B. After curing at room temperature, the peel strength (tensile rate of 50 mm/min) was 1.2×10^4 N/m (294 N/inch) and 7.5×10^3 N/m (192 N/inch) for aluminum and wood substrates, respectively. The lap shear strength (tensile rate of 12.7 mm/min) was 2.1×10^3 and 7.8×10^3 kPa for aluminium and wood substrates, respectively. To the best of our knowledge, in terms of adhesion force, our on-demand ductile adhesive elastomer tops the reported advanced ductile adhesive elastomers as illustrated by a summary of adhesion performance *vs*. materials shown in Figure 6.

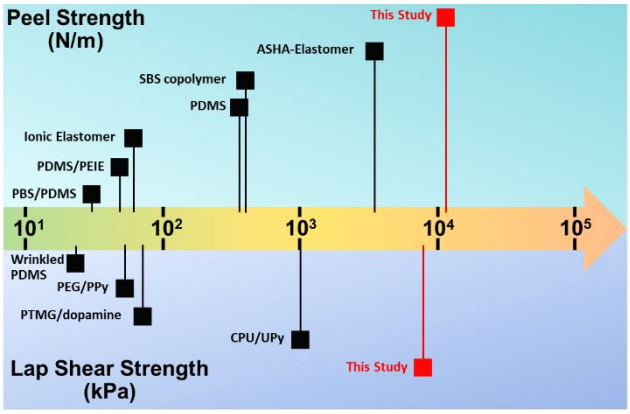

Figure 6. Summary of adhesion performance of currently reported advanced ductile adhesive elastomers, including the reported chemistries: ASHA-Elastomer [25], SBS copolymer [39], PDMS [21], ionic elastomer [48], PDMS/PEIE [49], PBS/PDMS [64], CPU/UPy [47], PTMG/dopamine [27], PEG/PPy [46], and wrinkled PDMS [50].

This ultra-high adhesion force provides a robust strategy to be utilized for applications on various substrate surfaces, and it can be explained for the following two reasons. First, the high mechanical robustness of the cured elastomer increases the cohesion strength. As measured by DMA, it showed an elastic modulus at least 10 times higher than regular rubbers, which provided reinforced cohesion during the peel test. Second, the ready-to-use precursor was pre-installed as a relatively liquid-like state that allowed the elastomer to adapt well to the texture roughness of the interface, significantly increasing the contact area. To examine the adhesion contribution from the matrix polymer, we also applied the peel test on the matrix polymer by itself with the same abovementioned method. As shown in Figure S10, the peel strength of the matrix polymer was only 1.8×10^3 N/m with clear cohesion failure observed (*vs* 1.2×10^4 N/m for our ductile adhesive elastomer). These results confirm the advantage of such a unique design that has a soft nature for efficient contact during installation and is mechanically robust after a force-triggered curing reaction.

The on-demand adhesion feature is of great potential for the prefab construction[101-103], as the precursor could be easily pre-installed on the module joints before triggering the cure, hence effectively reduce the labor and energy cost and alleviate the damage during transportation and installation. To demonstrate the potential application, we fabricated an example of a prefab tongue and grove joint that is commonly used with sheathings or boards with our elastomer precursor (Figure 7A). The joint was compressed for 30 seconds and cured under ambient conditions. Our high-resolution Instron tensile machine could barely pull the 5 cm-wide joints apart, as it exceeded the maximum load of 1000 N (Figure 7A). The ultra-high adhesion force was further illustrated in Figure 7B as the cured ductile adhesive elastomer could withstand the weight of 4 jugs of water, roughly 80 kg.

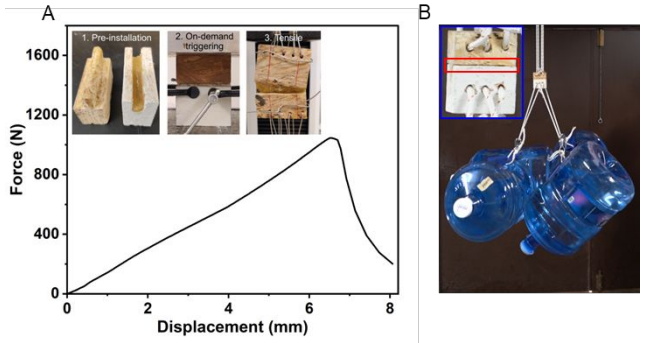

Figure 7. A) Tensile result of the bench-scale prefab joints connected by our cured elastomer, along with the protocol of setting up the bench-scale prefab joint. B) Illustration of the ultra-high adhesion performance of our ductile adhesive elastomer using the bench-scale prefab joints.

3. Conclusions

In summary, we report a novel design of ductile adhesive elastomers whose ultra-high adhesion strength can be easily triggered by an external force. The ready-to-use precursor was easily prepared with the encapsulated MDI-prepolymer as a reactive agent, PPG-diamine as curing agent, and polyacrylates as a matrix polymer. The encapsulated MDI-prepolymer was synthesized by partially crosslinking the MDI-prepolymer and the diameter of the microcapsules was adjustable. The polyacrylates matrix polymer improved the adhesion of the precursor and provided the advantage of self-healability. The on-demand adhesion feature was achieved by pre-installing the precursor onto a surface and easily triggered by a compression force. After curing, our ductile adhesive elastomer exhibited the peal strength and lap shear strength of 1.2×10^4 N/m and 7.8×10^3 kPa, respectively, which tops the reported adhesion force for advanced ductile elastomers. This ultra-high adhesion force is mainly due to the excellent surface contact of the liquid-like precursor and the high elastic modulus of the cured elastomer intrinsically reinforced by a two-phase design. We further demonstrated that the on-demand adhesion can be effectively used to seal joints between prefab components that are used in construction, as a prefab joint can withstand a force of at least 1000 N with a small 5 cm-wide joint. Our study sheds light on approaching the on-demand adhesion features for

advanced elastomer materials and provides predominant adhesion and flexibility over regular pressure-sensitive adhesives or ductile adhesive elastomers.

Conflicts of interest

The authors declare no conflict of interest.

Acknowledgments

This research was supported by the National Natural Science Foundation of China (grant no. 52373275 and 52303290). This work was funded by the Advanced Building Construction (ABC) Initiative under the Building Technologies Office (BTO) of the U.S. Department of Energy (DOE), under contract no. DE-AC05- 00OR22725. This manuscript was authored by UT-Battelle, LLC under contract no. DE-AC05-00OR22725 with the U.S. Department of Energy. The United States Government retains and the publisher, by accepting the article for publication, acknowledges that the United States Government retains a non-exclusive, paid-up, irrevocable, worldwide license to publish or reproduce the published form of this manuscript, or allow others to do so, for United States Government purposes. The Department of Energy will provide public access to these results of federally sponsored research in accordance with the DOE Public Access Plan (http://energy.gov/downloads/doe-public-access-plan).

References

1. G. Demirci, M. J. Niedźwiedź, N. Kantor-Malujdy and M. El Fray, *Polymers* 2022, **14 (9)**, 1822.
2. C. Ma, M.-G. Ma, C. Si, X.-X. Ji and P. Wan, *Advanced Functional Materials* 2021, **31 (22)**, 2009524.
3. Y. Li, J. Li, W. Li and H. Du, *Smart Materials and Structures* 2014, **23 (12)**, 123001.
4. C. S. Luo, P. Wan, H. Yang, S. A. A. Shah and X. Chen, *Advanced Functional Materials* 2017, **27 (23)**, 1606339.
5. Y. Guo, L. Liu, Y. Liu and J. Leng, *Advanced Intelligent Systems* 2021, **3 (10)**, 2000282.
6. S. Gao, M. Zhang, C. Gainaru, A. P. Sokolov, H. Yang and P.-F. Cao, *Matter* 2022, **5 (8)**, 2457-2460.
7. Q. Zhang, S. Niu, L. Wang, J. Lopez, S. Chen, Y. Cai, R. Du, Y. Liu, J.-C. Lai, L. Liu, C.-H. Li, X. Yan, C. Liu, J. B.-H. Tok, X. Jia and Z. Bao, *Advanced Materials* 2018, **30 (33)**, 1801435.
8. B. T. White and T. E. Long, *Macromolecular Rapid Communications* 2019, **40 (1)**, 1800521.
9. D. Zhang, Y. Tang, X. Gong, Y. Chang and J. Zheng, *SmartMat* 2023, e1160.
10. K. Parvathi, M. A. Al-Maghrabi, M. Subburaj and M. T. Ramesan, *Polymer Composites* 2021, **42 (9)**, 4586-4595.
11. C.-Y. Shi, Q. Zhang, C.-Y. Yu, S.-J. Rao, S. Yang, H. Tian and D.-H. Qu, *Advanced Materials* 2020, **32 (23)**, 2000345.
12. P. K. Behera, S. Mohanty and V. K. Gupta, *Polymer Chemistry* 2021, **12 (11)**, 1598-1621.
13. J. Huang, Y. Cai, C. Xue, J. Ge, H. Zhao and S.-H. Yu, *Nano Research* 2021, **14 (10)**, 3636-3642.
14. T. E. Long and J. Scheirs, *Modern Polyesters: Chemistry and Technology of Polyesters and Copolyesters*. **2005**, John Wiley & Sons.
15. Y. Xue, J. Lin, T. Wan, Y. Luo, Z. Ma, Y. Zhou, B. T. Tuten, M. Zhang, X. Tao and P. Song, *Advanced Science* 2023, 2207268.
16. Y. Lai, X. Kuang, P. Zhu, M. Huang, X. Dong and D. Wang, *Advanced Materials* 2018, **30 (38)**, 1802556.
17. X. Zhou, L. Wang, Z. Wei, G. Weng and J. He, *Advanced Functional Materials* 2019, **29 (34)**, 1903543.
18. J. H. Koo, D. C. Kim, H. J. Shim, T.-H. Kim and D.-H. Kim, *Advanced Functional Materials* 2018, **28 (35)**, 1801834.
19. L.-J. Yin, Y. Zhao, J. Zhu, M. Yang, H. Zhao, J.-Y. Pei, S.-L. Zhong and Z.-M. Dang, *Nature Communications* 2021, **12 (1)**, 4517.
20. E. Siéfert, E. Reyssat, J. Bico and B. Roman, *Nature Materials* 2019, **18 (1)**, 24-28.
21. A. M. Hubbard, W. Cui, Y. Huang, R. Takahashi, M. D. Dickey, J. Genzer, D. R. King and J. P. Gong, *Matter* 2019, **1 (3)**, 674-689.
22. Y. Yang, W. Zhan, R. Peng, C. He, X. Pang, D. Shi, T. Jiang and Z. Lin, *Advanced Materials* 2015, **27 (41)**, 6376-6381.
23. S. Liu, S. Wang, S. Xuan, S. Zhang, X. Fan, H. Jiang, P. Song and X. Gong, *ACS Applied Materials & Interfaces* 2020, **12 (13)**, 15675-15685.
24. J. Kang, D. Son, G.-J. N. Wang, Y. Liu, J. Lopez, Y. Kim, J. Y. Oh, T. Katsumata, J. Mun, Y. Lee, L. Jin, J. B.-H. Tok and Z. Bao, *Advanced Materials* 2018, **30 (13)**, 1706846.
25. Z. Zhang, N. Ghezawi, B. Li, S. Ge, S. Zhao, T. Saito, D. Hun and P.-F. Cao, *Advanced Functional Materials* 2021, **31 (4)**, 2006298.
26. J. Luo, Z. Demchuk, X. Zhao, T. Saito, M. Tian, A. P. Sokolov and P.-F. Cao, *Matter* 2022, **5 (5)**, 1391-1422.

27. Z. Xu, L. Chen, L. Lu, R. Du, W. Ma, Y. Cai, X. An, H. Wu, Q. Luo, Q. Xu, Q. Zhang and X. Jia, *Advanced Functional Materials* 2021, **31 (1)**, 2006432.
28. R. Du, Z. Xu, C. Zhu, Y. Jiang, H. Yan, H.-C. Wu, O. Vardoulis, Y. Cai, X. Zhu, Z. Bao, Q. Zhang and X. Jia, *Advanced Functional Materials* 2020, **30 (7)**, 1907139.
29. Y. Chen, Z. Tang, X. Zhang, Y. Liu, S. Wu and B. Guo, *ACS Applied Materials & Interfaces* 2018, **10 (28)**, 24224-24231.
30. Y. Chen, Z. Tang, Y. Liu, S. Wu and B. Guo, *Macromolecules* 2019, **52 (10)**, 3805-3812.
31. P. Wei and E. B. Pentzer, *Matter* 2022, **5 (8)**, 2479-2481.
32. P. Song and H. Wang, *Advanced Materials* 2020, **32 (18)**, 1901244.
33. Q. Ma, S. Liao, Y. Ma, Y. Chu and Y. Wang, *Advanced Materials* 2021, **33 (36)**, 2102096.
34. D. Zhang, Y. Tang, Y. Zhang, F. Yang, Y. Liu, X. Wang, J. Yang, X. Gong and J. Zheng, *Journal of Materials Chemistry A* 2020, **8 (39)**, 20474-20485.
35. F. Sun, Z. Li, S. Gao, Y. He, J. Luo, X. Zhao, D. Yang, T. Gao, H. Yang and P.-F. Cao, *ACS Applied Materials & Interfaces* 2022, **14 (22)**, 26014-26023.
36. X. Chu, R. Wang, H. Zhao, M. Kuang, J. Yan, B. Wang, H. Ma, M. Cui and X. Zhang, *ACS Applied Materials & Interfaces* 2022, **14 (14)**, 16631-16640.
37. K. Guk, G. Han, J. Lim, K. Jeong, T. Kang, E.-K. Lim and J. Jung, *Nanomaterials* 2019, **9 (6)**, 813.
38. Y. Fang and J. Xia, *ACS Applied Materials & Interfaces* 2022, **14 (33)**, 38398-38408.
39. N. Sato, A. Murata, T. Fujie and S. Takeoka, *Soft Matter* 2016, **12 (45)**, 9202-9209.
40. L. Meng, J. He and C. Pan, *Materials* 2022, **15 (7)**, 2548.
41. A. B. Croll, N. Hosseini and M. D. Bartlett, *Advanced Materials Technologies* 2019, **4 (8)**, 1900193.
42. R. Coulson, C. J. Stabile, K. T. Turner and C. Majidi, *Soft Robotics* 2022, **9 (2)**, 189-200.
43. H. Iwasaki, F. Lefevre, D. D. Damian, E. Iwase and S. Miyashita, *IEEE Robotics and Automation Letters* 2020, **5 (2)**, 2015-2022.
44. Z. Ma, G. Bao and J. Li, *Advanced Materials* 2021, **33 (24)**, 2007663.
45. M. Runciman, A. Darzi and G. P. Mylonas, *Soft Robotics* 2019, **6 (4)**, 423-443.
46. J. Chen, J. Liu, T. Thundat and H. Zeng, *ACS Applied Materials & Interfaces* 2019, **11 (20)**, 18720-18729.
47. M. W. M. Tan, G. Thangavel and P. S. Lee, *Advanced Functional Materials* 2021, **31 (34)**, 2103097.
48. L. Wang, Y. Wang, S. Yang, X. Tao, Y. Zi and W. A. Daoud, *Nano Energy* 2022, **91**, 106611.
49. S. H. Jeong, S. Zhang, K. Hjort, J. Hilborn and Z. Wu, *Advanced Materials* 2016, **28 (28)**, 5830-5836.
50. C.-H. Lin, C.-Y. Huang, J.-Y. Ho and H.-Y. Hsueh, *ACS Applied Materials & Interfaces* 2020, **12 (19)**, 22365-22377.
51. B. J. Blaiszik, S. L. B. Kramer, S. C. Olugebefola, J. S. Moore, N. R. Sottos and S. R. White, *Annual Review of Materials Research* 2010, **40 (1)**, 179-211.
52. D. Y. Zhu, M. Z. Rong and M. Q. Zhang, *Progress in Polymer Science* 2015, **49-50**, 175-220.
53. K. Wazarkar, D. Patil, A. Rane, D. Balgude, M. Kathalewar and A. Sabnis, *RSC Advances* 2016, **6 (108)**, 106964-106979.
54. V. Nedovic, A. Kalusevic, V. Manojlovic, S. Levic and B. Bugarski, *Procedia Food Science* 2011, **1**, 1806-1815.
55. C. J. Martínez Rivas, M. Tarhini, W. Badri, K. Miladi, H. Greige-Gerges, Q. A. Nazari, S. A. Galindo Rodríguez, R. Á. Román, H. Fessi and A. Elaissari, *International Journal of Pharmaceutics* 2017, **532 (1)**, 66-81.
56. M. Villiou, J. I. Paez and A. del Campo, *ACS Applied Materials & Interfaces* 2020, **12 (34)**, 37862-37872.
57. W. Sliwka, *Angewandte Chemie International Edition in English* 1975, **14 (8)**, 539-550.
58. Q. Lu, Z. Yang, X. Meng, Y. Yue, M. A. Ahmad, W. Zhang, S. Zhang, Y. Zhang, Z. Liu and W. Chen, *Advanced Functional Materials* 2021, **31 (23)**, 2100151.
59. S. M. Jee, C.-H. Ahn, J. H. Park, T. A. Kim and M. Park, *Composites Part B: Engineering* 2020, **202**, 108438.
60. M. M. Caruso, B. J. Blaiszik, S. R. White, N. R. Sottos and J. S. Moore, *Advanced Functional Materials* 2008, **18 (13)**, 1898-1904.
61. S. H. Cho, H. M. Andersson, S. R. White, N. R. Sottos and P. V. Braun, *Advanced Materials* 2006, **18 (8)**, 997-1000.
62. M. J. Shin, Y. J. Shin, S. W. Hwang and J. S. Shin,

Journal of Applied Polymer Science 2013, **129 (3)**, 1036-1044.
63. Y. Zhang, J. Yu, H. N. Bomba, Y. Zhu and Z. Gu, *Chemical Reviews* 2016, **116 (19)**, 12536-12563.
64. J. Giro-Paloma, C. Barreneche, M. Martínez, B. Šumiga, A. I. Fernández and L. F. Cabeza, *Renewable Energy* 2016, **85**, 732-739.
65. H. Zhao, X. Fei, L. Cao, B. Zhang and X. Liu, *Materials* 2019, **12 (3)**, 393.
66. A. Ghaemi, A. Philipp, A. Bauer, K. Last, A. Fery and S. Gekle, *Chemical Engineering Science* 2016, **142**, 236-243.
67. A. P. Esser-Kahn, S. A. Odom, N. R. Sottos, S. R. White and J. S. Moore, *Macromolecules* 2011, **44 (14)**, 5539-5553.
68. J. Yang, M. W. Keller, J. S. Moore, S. R. White and N. R. Sottos, *Macromolecules* 2008, **41 (24)**, 9650-9655.
69. P.-F. Cao, B. Li, T. Hong, K. Xing, D. N. Voylov, S. Cheng, P. Yin, A. Kisliuk, S. M. Mahurin, A. P. Sokolov and T. Saito, *ACS Applied Materials & Interfaces* 2017, **9 (31)**, 26483-26491.
70. T. Yin, M. Z. Rong, M. Q. Zhang and G. C. Yang, *Composites Science and Technology* 2007, **67 (2)**, 201-212.
71. J. S. Nakka, K. M. B. Jansen and L. J. Ernst, *Journal of Polymer Research* 2011, **18 (6)**, 1879-1888.
72. G. Yang, S.-Y. Fu and J.-P. Yang, *Polymer* 2007, **48 (1)**, 302-310.
73. E. Urbaczewski-Espuche, J. Galy, J.-F. Gerard, J.-P. Pascault and H. Sautereau, *Polymer Engineering & Science* 1991, **31 (22)**, 1572-1580.
74. S. J. McCarthy, G. F. Meijs, N. Mitchell, P. A. Gunatillake, G. Heath, A. Brandwood and K. Schindhelm, *Biomaterials* 1997, **18 (21)**, 1387-1409.
75. M. Strankowski, D. Włodarczyk, Ł. Piszczyk and J. Strankowska, *Journal of Spectroscopy* 2016, **2016**, 7520741.
76. Z. Wen, M. K. McBride, X. Zhang, X. Han, A. M. Martinez, R. Shao, C. Zhu, R. Visvanathan, N. A. Clark, Y. Wang, K. Yang and C. N. Bowman, *Macromolecules* 2018, **51 (15)**, 5812-5819.
77. V. A. Gabriel and M. A. Dubé, *Macromolecular Reaction Engineering* 2019, **13 (2)**, 1800057.
78. M. Tang, P. Zheng, K. Wang, Y. Qin, Y. Jiang, Y. Cheng, Z. Li and L. Wu, *Journal of Materials Chemistry A* 2019, **7 (48)**, 27278-27288.
79. J. Li, A. Celiz, J. Yang, Q. Yang, I. Wamala, W. Whyte, B. Seo, N. Vasilyev, J. Vlassak and Z. Suo, *Science* 2017, **357 (6349)**, 378-381.
80. D. F. S. Saldanha, C. Canto, L. F. M. da Silva, R. J. C. Carbas, F. J. P. Chaves, K. Nomura and T. Ueda, *International Journal of Adhesion and Adhesives* 2013, **47**, 91-98.
81. L. Wang, G. Gao, Y. Zhou, T. Xu, J. Chen, R. Wang, R. Zhang and J. Fu, *ACS Applied Materials & Interfaces* 2019, **11 (3)**, 3506-3515.
82. J. S. Santana, E. S. Cardoso, E. R. Triboni and M. J. Politi, *Polymers* 2021, **13 (24)**, 4393.
83. J. D. Ferry, *Viscoelastic Properties of Polymers*. **1980**, John Wiley & Sons.
84. T. Hwang, Z. Frank, J. Neubauer and K. J. Kim, *Scientific Reports* 2019, **9 (1)**, 9658.
85. M. Hao, L. Li, S. Wang, F. Sun, Y. Bai, Z. Cao, C. Qu and T. Zhang, *Microsystems & Nanoengineering* 2019, **5 (1)**, 9.
86. T. Noguchi, M. Endo, K. Niihara, H. Jinnai and A. Isogai, *Composites Science and Technology* 2020, **188**, 108005.
87. B. M. Boyle, O. Heinz, G. M. Miyake and Y. Ding, *Macromolecules* 2019, **52 (9)**, 3426-3434.
88. B. D. B. Tiu, P. Delparastan, M. R. Ney, M. Gerst and P. B. Messersmith, *Angewandte Chemie International Edition* 2020, **59 (38)**, 16616-16624.
89. A. Zosel, *The Journal of Adhesion* 1989, **30 (1-4)**, 135-149.
90. T. L. Gordon and M. E. Fakley, *International Journal of Adhesion and Adhesives* 2003, **23 (2)**, 95-100.
91. F. P. M. Mercx, A. Benzina, A. D. van Langeveld and P. J. Lemstra, *Journal of Materials Science* 1993, **28 (3)**, 753-759.
92. Z. Zhang, J. Luo, S. Zhao, S. Ge, J.-M. Y. Carrillo, J. K. Keum, C. Do, S. Cheng, Y. Wang, A. P. Sokolov and P.-F. Cao, *Matter* 2022, **5 (1)**, 237-252.
93. Y. Zheng, R. Kiyama, T. Matsuda, K. Cui, X. Li, W. Cui, Y. Guo, T. Nakajima, T. Kurokawa and J. P. Gong, *Chemistry of Materials* 2021, **33 (9)**, 3321-3334.
94. Y. Zhuo, Z. Xia, Y. Qi, T. Sumigawa, J. Wu, P. Šesták, Y. Lu, V. Håkonsen, T. Li, F. Wang, W. Chen, S. Xiao, R. Long, T. Kitamura, L. Li, J. He and Z. Zhang, *Advanced Materials* 2021, **33 (23)**, 2008523.
95. S. Sun, M. Li and A. Liu, *International Journal of Adhesion and Adhesives* 2013, **41**, 98-106.

96. S. Mapari, S. Mestry and S. T. Mhaske, *Polymer Bulletin* 2021, **78 (7)**, 4075-4108.
97. R. Jovanović and M. A. Dubé, *Journal of Macromolecular Science, Part C* 2004, **44 (1)**, 1-51.
98. B. T. Poh and H. K. Kwo, *Polymer-Plastics Technology and Engineering* 2007, **46 (10)**, 1021-1024.
99. B. T. Poh and H. K. Kwo, *Journal of Applied Polymer Science* 2007, **105 (2)**, 680-684.
100. I. Khan and B. T. Poh, *Journal of Polymers and the Environment* 2011, **19 (3)**, 793-811.
101. S. G. Naoum, *International Journal of Productivity and Performance Management* 2016, **65 (3)**, 401-421.
102. K. M. A. El-Abidi and F. E. M. Ghazali, *Applied Mechanics and Materials* 2015, **802**, 668-675.
103. F. E. Boafo, J.-H. Kim and J.-T. Kim, *Sustainability* 2016, **8 (6)**, 558.